Local translation of yeast *ERG4* mRNA at the endoplasmic reticulum requires the brefeldin A resistance protein Bfr1

SRINIVAS MANCHALU,[1] NITISH MITTAL,[2] ANNE SPANG,[2] and RALF-PETER JANSEN[1]

[1]Interfaculty Institute of Biochemistry, University of Tübingen, Tübingen 72076, Germany
[2]Biozentrum, University of Basel, Basel 4056, Switzerland

ABSTRACT

Brefeldin A resistance factor 1 (Bfr1p) is a nonessential RNA-binding protein and multicopy suppressor of brefeldin A sensitivity in *Saccharomyces cerevisiae*. Deletion of *BFR1* leads to multiple defects, including altered cell shape and size, change in ploidy, induction of P-bodies and chromosomal missegregation. Bfr1p has been shown to associate with polysomes, binds to several hundred mRNAs, and can target some of them to P-bodies. Although this implies a role of Bfr1p in translational control of mRNAs, its molecular function remains elusive. In the present study, we show that mutations in RNA-binding residues of Bfr1p impede its RNA-dependent colocalization with ER, yet do not mimic the known cellular defects seen upon *BFR1* deletion. However, a Bfr1 RNA-binding mutant is impaired in binding to *ERG4* mRNA, which encodes an enzyme required for the final step of ergosterol biosynthesis. Consistently, *bfr1Δ* strains show a strong reduction in Erg4p protein levels, most likely because of degradation of misfolded Erg4p. Polysome profiling of *bfr1Δ* or *bfr1* mutant strains reveals a strong shift of *ERG4* mRNA to polysomes, consistent with a function of Bfr1p in elongation or increased ribosome loading. Collectively, our data reveal that Bfr1 has at least two separable functions: one in RNA binding and cotranslational protein translocation into the ER and one in ploidy control or chromosome segregation.

Keywords: RNA-binding protein; yeast; endoplasmic reticulum; brefeldin A resistance; ribosomal occupancy; RNA-protein interaction

INTRODUCTION

Function and lifetime of mRNAs are largely controlled by RNA-binding proteins (RBPs) that can regulate RNA folding, stability, translation, localization, or access by other proteins (Dreyfuss et al. 2002; Lunde et al. 2007; Björk and Wieslander 2017; Neriec and Percipalle 2018). These proteins can bind RNA cotranscriptionally at birth and dynamically associate/dissociate throughout the lifetime of mRNAs. RNA recognition and binding generally occurs via RNA-binding domains (RBDs). Common RBDs include the RNA recognition motif (RRM; Oubridge et al. 1994), the heterologous nuclear RBP K homology (KH) domain (Lewis et al. 2000), the double-stranded RNA-binding domain (dsRBD; Ryter and Schultz 1998), or zinc-finger domains (Lu et al. 2003); for a detailed and more complete list, see Auweter et al. (2006) and Lunde et al. (2007). However, high-throughput RNA-binding studies have revealed a large number of RBPs lacking known RBDs, implicating the presence of even more RBPs than previously anticipated (Baltz et al. 2012; Castello et al. 2012, 2015; Kwon et al. 2013; Beckmann et al. 2015; Hentze et al. 2018). RNA binding of these proteins frequently occurs via intrinsically disordered regions (IDRs; Hentze et al. 2018) or nucleotide-binding sites (Castello et al. 2015, 2016). Many of these proteins, like some enzymes, have functions additional to RNA binding. Furthermore, in many cases, we do not know the biological function of RNA binding or even their RNA targets.

The 55-kDa budding yeast Bfr1 protein is a nonessential RBP lacking common RBDs. The gene had been originally identified in a screen for genes relieving the growth defect seen in yeast cells carrying a mutation in *SEC21* if exposed to the drug brefeldin A (Jackson and Képès 1994) and hence named brefeldin A resistance factor 1 (*BFR1*). Because brefeldin A inhibits transport out of the Golgi apparatus, this early work suggested that Bfr1p is involved in membrane trafficking (Jackson and Képès 1994). However, later studies revealed a role for Bfr1p in mRNA metabolism (Lang et al. 2001). Bfr1p cofractionates with polysomes,

Corresponding author: ralf.jansen@uni-tuebingen.de
Article is online at http://www.rnajournal.org/cgi/doi/10.1261/rna.072017.119.

implying a function in translation. In addition, it associates with RNA–protein particles (RNPs) that contain the mRNA-binding protein Scp160p (Lang and Fridovich-Keil 2000) and the ribosome-associated protein Asc1p (Sezen et al. 2009). Copurification of Bfr1p with mRNPs is independent of Scp160p, but Bfr1p is required for Scp160p's association with polysomes (Lang et al. 2001). Consistent with its putative role in translation, Bfr1p is present in the cytoplasm but also localizes to the endoplasmic reticulum (ER), possibly because of its interaction with polyribosomes translating membrane or secreted proteins (Lang et al. 2001).

Potential RNA targets of Bfr1p have been revealed in several studies using RBP immunoprecipitation coupled with microarray analysis (RIP-Chip; Hogan et al. 2008), cross-linking and immunoprecipitation (CLIP; Mitchell et al. 2013), or RNA tagging (Lapointe et al. 2015). All studies concurrently reported that Bfr1p binds to several hundred different mRNAs. The set of Bfr1p-associated mRNAs largely overlaps with those that encode proteins translated at the ER (Jan et al. 2014; Lapointe et al. 2015). A similar observation had been made for Scp160p (Hogan et al. 2008; Lapointe et al. 2015), supporting the idea that the protein is implicated in ER-based translation.

In addition, Bfr1p functions in stress-related mRNA decay. During glucose depletion, Bfr1p relocates to P-bodies at a late stage of P-body formation (Simpson et al. 2014). It is also required for targeting of mRNAs to P-bodies at a late phase of stress. In unstressed cells, Bfr1p and Scp160 act as negative regulators of P-body formation, probably by protecting mRNA at polysomes (Weidner et al. 2014). Lack of any of these proteins results in P-body-like structures even under optimal growth conditions (Weidner et al. 2014). Loss of Bfr1p additionally leads to changes in the cell ploidy (Jackson and Képès 1994). Such ploidy changes could be the result of chromosome missegregation due to a failure to build a functional mitotic bipolar spindle. Monopolar spindles can arise from defects in spindle pole body (SPB) duplication, and the SPB component Bbp1p has been reported to bind to Bfr1p (Xue et al. 1996). In addition, Bfr1p interacts with the SESA (Smy2-Eap1-Scp160-Asc1) network that controls spindle pole duplication (Sezen et al. 2009).

All previous studies that reported on phenotypes associated with loss of Bfr1p were performed with *BFR1* deletion cells. Because the loss of Bfr1p results in alterations of the genome (Jackson and Képès 1994), it remained unclear if the observed effects are a direct consequence of Bfr1p loss and to what extent loss of RNA binding or misregulation of Bfr1p targets contribute to the phenotypes. Therefore, we generated Bfr1p mutants with point mutations in known RNA-binding sites in order to establish a link between mRNA binding, brefeldin A resistance, ploidy control, and translation. Here, we demonstrate that RNA binding is required for Bfr1p function in translational regulation or protein translocation of *ERG4* that encodes an ergosterol-synthesizing enzyme, that, in *bfr1* mutants, Erg4p becomes a substrate for the ERAD pathway because of its misfolding, and that RNA-binding of Bfr1p is independent of its role in ploidy maintenance.

RESULTS

RNA binding of Bfr1p is required for its localization to the ER

The noncanonical RBP Bfr1p is involved in several cellular processes including transfer and retention of mRNAs to P-bodies (Simpson et al. 2014; Weidner et al. 2014), translation (Lang et al. 2001), and response to functional failure of the yeast SPB or kinetochore (Sezen et al. 2009; Low et al. 2014). We generated *bfr1* mutants in order to address the question of whether RNA binding is required for all processes. Because Bfr1p lacks canonical RBDs, we made alanine substitutions at amino acid positions that had previously been identified to cross-link with RNA in vivo (Supplemental Fig. S1; Kramer et al. 2014; Lapointe et al. 2015). Out of the six RNA contact sites that have been described, we initially focused on the two amino acids (K138, F239) that are most highly conserved in Bfr1p among different yeast species (Fig. 1A; Supplemental Fig. S1). In addition, we generated a shorter Bfr1p variant that lacks the third coiled-coil domain, which is devoid of any identified RNA contact sites (Kramer et al. 2014). When expressed as carboxy-terminal GFP fusion proteins in a *bfr1Δ* yeast strain, Bfr1p mutant proteins with point mutations in two cross-link sites (K139 or F293) or in all six sites are expressed similarly (Fig. 1B,C) as endogenous full-length Bfr1p (Bfr1p WT FL). Similar results were obtained for the deletion of mutant Bfr1p(1–397). In exponentially growing yeast cells, Bfr1p is located in the cytoplasm and at the ER (Lang et al. 2001), which is recapitulated by our Bfr1-GFP fusion protein (Fig. 1D,E). Whereas deletion of the third coiled-coil domain does not affect this distribution, mutation of all six conserved RNA cross-link sites as well as also the single exchange of F239A results in a partial loss of Bfr1p from the ER as determined by live-cell imaging and subcellular fractionation (Fig. 1D,E). The majority of wild-type Bfr1p cosediments with a membrane fraction containing ER as judged by the distribution of the ER marker Sec61p (Fig. 1F). Similarly, the signal of Bfr1p(1–397) in the membrane fraction is also more prominent than in the cytoplasmic fraction. In contrast, the ratio of Bfr1p between the membrane and cytoplasmic fraction is inversed for the *bfr1mut6A* mutant (Fig. 1F). Out of all single point mutations, F239 is the only cross-link site for which a mutation affects ER localization. Single mutations in each of the other five sites result in no change in Bfr1p distribution (Supplemental Fig. S2). To investigate whether the loss of ER localization of *bfr1mut6A* and *bfr1mutF293A* proteins

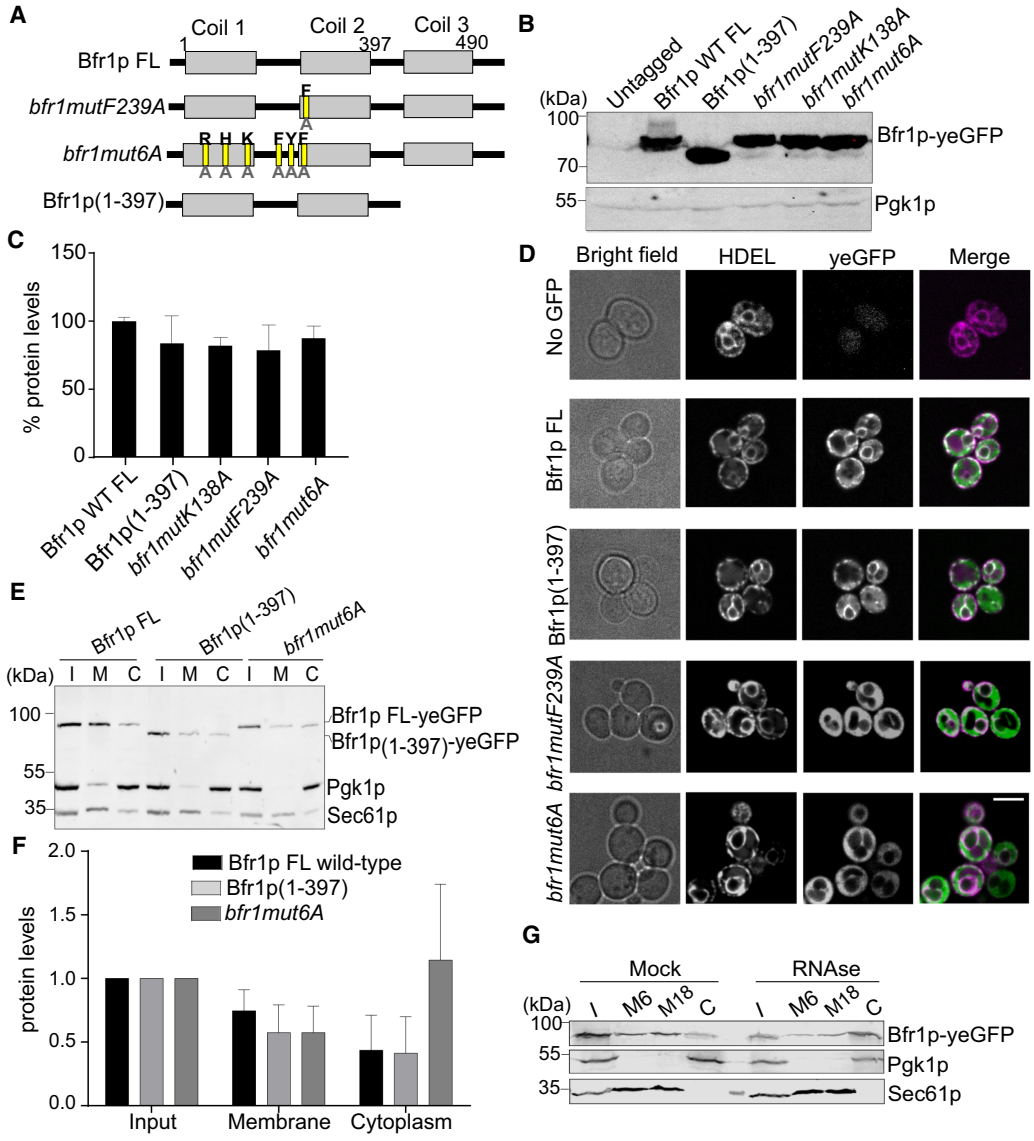

FIGURE 1. Mutations in RNA-binding residues of Bfr1p affects the Bfr1p-ER localization. (*A*) Schematic view of the Bfr1p constructs used in this study. All four constructs were fused to a carboxy-terminal yeGFP and integrated into the genomic *BFR1* locus. RNA-binding residues R38, H79, K138, F211, Y225, and F239 were replaced with alanine, and mutant *bfr1mut6A* contains all six mutations. Bfr1p(1–397) is a truncation lacking the third coiled-coil. (*B*) Equal expression of Bfr1p in various mutants of RNA-binding residues. Total cell lysates from the yeGFP-tagged Bfr1p full-length (WT FL), Bfr1p(1–397), *bfr1mutF239A*, *bfr1mutK138A*, and *bfr1mut6A* were analyzed by western blotting. Pgk1p serves as a loading control. (*C*) Quantification of Bfr1p levels. Data displayed as percentage protein levels compared to the wild type from three biological replicates. Normalization to Pgk1p was performed for each strain before normalization to Bfr1p wild-type levels were made. Error bars show ±SD. (*D*) Intracellular distribution of yeGFP-tagged Bfr1p constructs. Plasmid-expressed HDEL-DsRed serves as an ER marker. Bfr1p variants of mutants *bfr1mutF239A* and *bfr1mut6A* show loss of colocalization between Bfr1p and the ER. Scale bar, 8 µm. (*E*) Distribution of Bfr1p constructs in subcellular fractionation. (I) input, (M) membrane fraction (pellet from 18,000*g*), (C) cytoplasmic fraction (supernatant from 18,000*g*). Pgk1p serves as cytosolic and Sec61p as ER markers. (*F*) Quantification of subcellular fractionation of yeGFP-tagged Bfr1p constructs. Data are displayed as relative protein levels. Protein in the membrane fraction was normalized to Sec61p and in cytoplasmic fraction to Pgk1p. Results stem from three biological replicates. Error bars show ±SD. (*G*) Redistribution of Bfr1p between the membrane and cytosolic fractions upon RNase treatment. (M6) membrane fraction (pellet from 6000*g*), (M18) membrane fraction (pellet from 18,000*g*), and (C) cytoplasmic fraction (supernatant from 18,000*g*).

is due to loss of RNA binding, we followed the distribution of wild-type Bfr1p in the subcellular distribution in lysates treated with RNase A (Fig. 1G). RNA degradation results in a similar redistribution of Bfr1p from the membrane fractions to a cytosolic fraction—the same as that observed for the mutant proteins. This suggests that the RNA-binding ability of Bfr1p is required for its localization to the ER in yeast.

Because deletion of *BFR1* is associated with various phenotypes, we also tested if *bfr1mut6A* or *bfr1mutF293A* affect ploidy maintenance (Jackson and Képès 1994; Xue et al. 1996), resistance to brefeldin A (Jackson and Képès 1994), or premature formation of P-bodies (Weidner et al. 2014). As described before, complete loss of *BFR1* results in a ploidy shift from 1N to 2N as exemplified by the shift of DNA peaks from 1C/2C (haploid) to 2C/4C (diploid) in flow cytometry analysis (Fig. 2A; Supplemental Fig. S3). However, a similar shift is not seen in the tested mutants (Fig. 2A). Overexpression of *BFR1* has been demonstrated to rescue the brefeldin A sensitivity of a yeast mutant lacking the *ERG6* gene (Graham et al. 1993; Shah and Klausner 1993). Because all tested *bfr1* point mutants including mutant *bfr1mut6A* are still able to rescue *erg6Δ* to a similar level as the wild type (Fig. 2B), we conclude that none of these sites are important for suppression of the brefeldin A sensitivity in *erg6Δ*. Similarly, none of the RNA-binding mutants lead to the occurrence of premature P-bodies is observed in *bfr1Δ* cells. Formation of P-bodies in wild-type cells or *bfr1Δ* cells expressing various Bfr1p-GFP variants was assessed by coexpression of Edc3p-mCherry, a bona fide P-body marker (Weidner et al. 2014). Formation of Edc3p-positive cytoplasmic foci in wild-type cells is induced by transferring cells into medium lacking glucose (Fig. 2C, right panels), a potent inducer of P-bodies. Whereas *bfr1Δ* cells form Edc3p foci also in the presence of glucose, expression of full-length Bfr1p or Bfr1p RNA-binding mutants rescues this phenotype (Fig. 2C, left panels).

Taken together, point mutations in F239 or the six amino acids that form cross-links to RNA affect the intracellular distribution of Bfr1p—in particular, ER localization—but this ER localization of Bfr1p is not required for ploidy maintenance, brefeldin A sensitivity, or P-body formation, indicating that RNA binding might not be required for these functions of Bfr1p.

Colocalization of the Bfr1p mRNA target *ERG4* with ER is independent of Bfr1p

Several hundred mRNAs have been identified that are potential binding partners of Bfr1p and translated at the ER (Hogan et al. 2008; Mitchell et al. 2013; Lapointe et al. 2015), but it has not yet been addressed how Bfr1p affects their function. We, therefore, addressed the physiological changes of potential Bfr1p RNA targets upon mutation of its RNA contact sites. Because Bfr1p is enriched at the ER where mRNAs encoding membrane or secreted proteins are translated, we focused on five Bfr1p targets that encode proteins of these groups and whose functions have been linked to described phenotypes of *bfr1Δ* or Bfr1p overexpression (Lai et al. 1994; Entian et al. 1999; Zweytick et al. 2000; Beh et al. 2001; Gillingham and Munro 2003; Setty et al. 2003). These candidates were selected by comparing the top identified Bfr1p binders from two studies (Hogan et al. 2008; Lapointe et al. 2015). Based on Bfr1p's suppression of the growth inhibition by brefeldin A (Jackson and Képès 1994), the subsequent selection focused on mRNAs encoding ER- or Golgi-localized proteins (*ERG4*, *RUD3*, *SGM1*), proteins involved in ER-Golgi transport (*IMH1*), or those involved in sterol biosynthesis (*ERG4*) or binding (*OSH7*). Because the loss of Bfr1p has been linked to premature P-body formation (Weidner et al. 2014), we first tested if the loss of *BFR1*, deletion of the last coiled-coil domain, or mutations in RNA contact sites affect the stability of the five selected mRNAs. As judged by qRT-PCR from total RNA isolates, none of the five tested mRNAs showed a significant change in their levels (Fig. 3A). We verified whether these mRNAs are bona fide targets of Bfr1p and whether the introduced mutations of Bfr1p RNA-binding sites interfere with their binding, and we investigated two mRNAs, *OSH7* and *ERG4*. We performed coimmunoprecipitation using GFP-tagged versions of wild-type Bfr1p, *bfr1mut6A*, and Bfr1p(1–397), as well as a control RNA-binding GFP fusion protein, Khd1p (Hasegawa et al. 2008; Syed et al. 2018). *MID2*, an mRNA bound by Khd1p (Syed et al. 2018) served as control mRNA. Only *ERG4* mRNA showed an enrichment in a Bfr1-GFP pull-down, whereas *OSH7* was even more enriched in GFP-Khd1p pull-downs than by Bfr1-GFP pull-downs (Fig. 3B). Importantly, *ERG4* enrichment is lost in the *bfrmut6A* mutant, supporting the idea that this mRNA is a direct target of Bfr1p.

We have previously shown that RBPs like She2p (Schmid et al. 2006; Fundakowski et al. 2012) or Khd1p (Syed et al. 2018) are required for ER localization of bound mRNAs. Because Bfr1p colocalizes with ER and *ERG4* encodes a membrane protein that is supposed to be synthesized from an ER-associated mRNA, we next tested whether the loss of *BFR1* interferes with ER association of *ERG4*. *ERG4* mRNA was tagged with 12 MS2 stem–loops using the recently published improved MS2-tagging system (Tutucci et al. 2018) and localization of the mRNA was followed by coexpression of a GFP-MCP (MS2 coat protein) fusion protein. ER was detected by a fusion of the transmembrane domain of Scs2p (Scs2-TMD) and 2× RFP (Loewen et al. 2007). In the majority of wild-type cells (86.6 ± 3.6%) and cells lacking *BFR1* (84 ± 2.6%), *ERG4-MS2* RNA particles were detected at or very close to the ER marker (Fig. 3C,D), indicating that Bfr1p is not required for ER association of *ERG4* mRNA.

Synthesis of the sterol reductase Erg4p depends on Bfr1p

In parallel to the RNA localization experiments, we wanted to determine if the loss of *BFR1* impacts Erg4 protein localization. The C-24(28) sterol reductase Erg4p is a seven-transmembrane domain protein that catalyzes the final

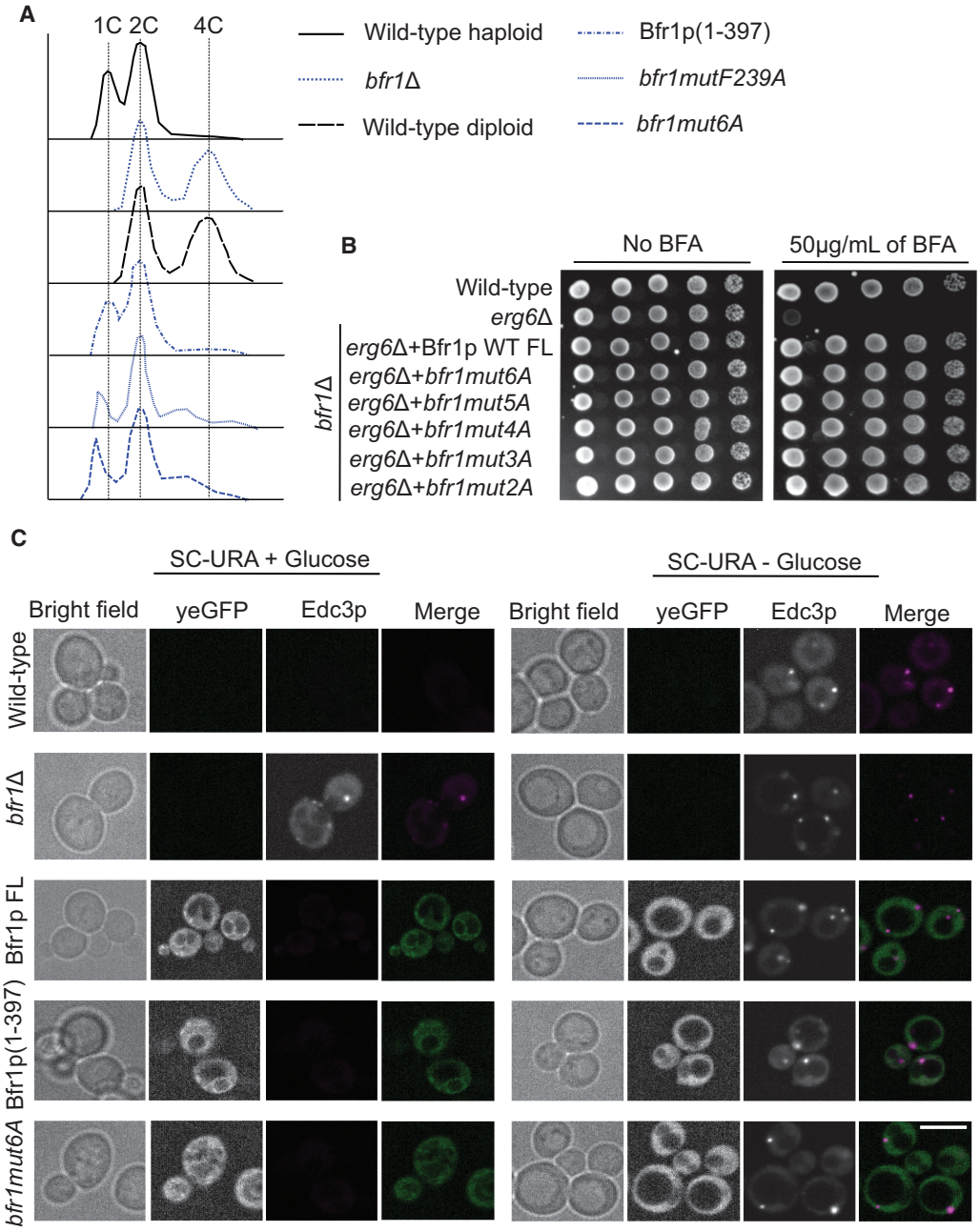

FIGURE 2. Bfr1p-associated phenotypes are independent of Bfr1p–RNA interactions. (*A*) Flow cytometry analysis of Bfr1p variants showing that ploidy is not changed by the mutations in RNA-binding residues of Bfr1p. Histograms show plots of DNA content after propidium iodide staining. (*B*) Brefeldin A sensitivity of *erg6Δ* is rescued by overexpression of wild-type Bfr1p and RNA-binding mutants. Bfr1p mutants (*bfr1mut5A*: *R38A*, *K138A*, *F211A*, *Y225A*, *F239A*; *bfr1mut4A*: *R38A*, *K138A*, *F211A*, *F239A*; *bfr1mut3A*: *R38A*, *K138A*, *F239*; *bfr1mut2A*: *K138A*, *F239A*) were expressed from YEplac181 (*LEU2*) plasmids in cells deleted for *BFR1* (*bfr1::HIS3MX6*) and *ERG6* (*erg6::KanMX4*). Wild-type and *erg6Δ* cells with empty YEplac181 plasmids served as controls. Logarithmically growing cells were serially diluted, plated on dropout (*-leucine*) agar with or without 50 µg/mL brefeldin A, and grown for 72 h at 30°C. (*C*) Premature P-bodies are not induced by RNA-binding mutations of Bfr1p. Images were collected from logarithmically growing cells in dropout media lacking uracil that are shifted for 30 min to media with or without glucose to induce P-bodies. Plasmid-expressed Edc3p-mCherry serves as P-body marker. Unlike a *BFR1* deletion, neither RNA-binding mutations nor Bfr1p(1–397) show any P-body foci in cells growing in glucose-containing medium. Scale bar, 5 µm.

step of ergosterol biosynthesis in the yeast ER (Zweytick et al. 2000). Consistent with previous observations, a carboxy-terminal fusion of Erg4p with yeast enhanced GFP (yeGFP) colocalizes with an ER marker (HDEL-DSRED; Bevis and Glick 2002), predominantly with perinuclear ER (Fig. 4A). Although mRNA localization is unaffected, the protein level appears to be drastically reduced and no ER colocalization was detected in *bfr1Δ* cells (Fig. 4A,B).

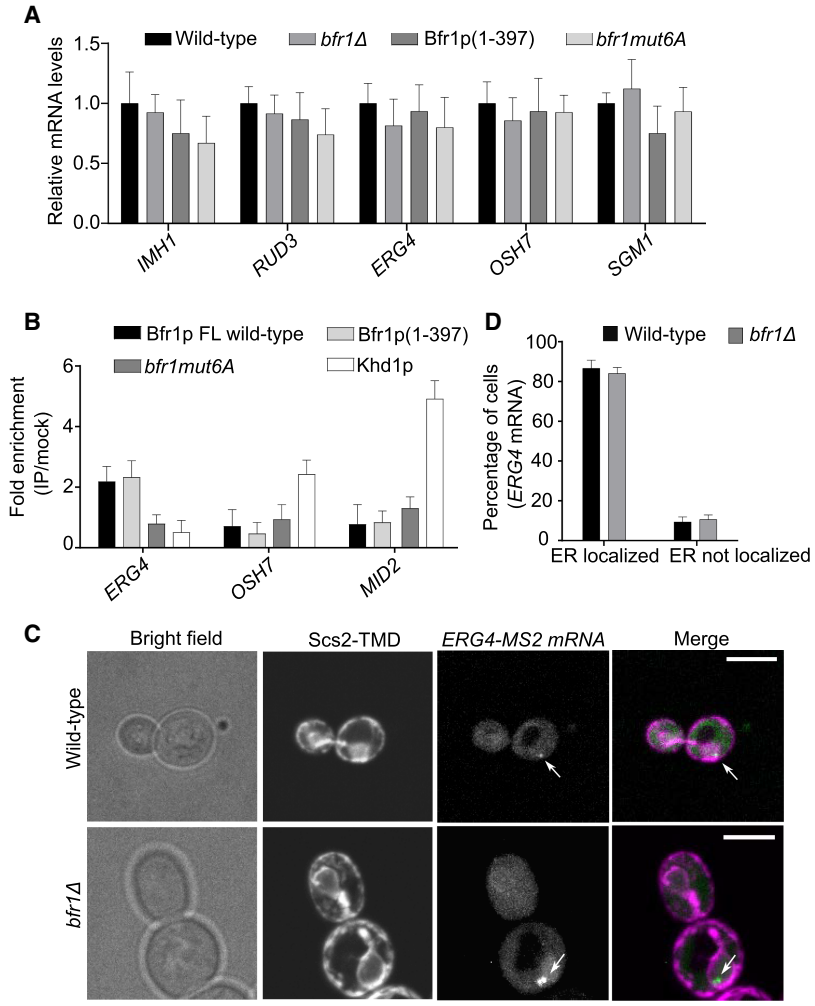

FIGURE 3. Bfr1p is not required for the association of *ERG4* mRNA with ER. (*A*) Mutations in RNA-binding sites in Bfr1p do not affect target mRNA levels. Quantification of mRNA levels of *IMH1*, *RUD3*, *ERG4*, *OSH7*, and *SGM1* by qRT-PCR. Data are presented as mean values from three independent experiments with ±SD. (*B*) *ERG4* mRNA binding is strongly affected in *bfr1mut6A*. RNA binding of full-length Bfr1p (FL wild type), Bfr1p(1–397), and *bfr1mut6A* is assessed by coimmunoprecipitation of *ERG4* and *OSH7* mRNAs and qRT-PCR. *MID2* mRNA serves as a nontarget for Bfr1p. Data are presented as mean values from three biological and two technical replicates, each with ±SD. (*C*) *ERG4* mRNA association with ER is independent of Bfr1p. Representative images of cells expressing MS2-tagged *ERG4* mRNA in wild-type and *bfr1*Δ. Scs2-TMD-2× RFP serves as an ER marker. White arrows indicate *ERG4* mRNA particles. Scale bar, 8 µm. (*D*) Quantification of *ERG4* mRNA colocalization with ER in wild type and *bfr1*Δ. Data are presented as mean values from at least 100 cells from three biological replicates with ±SD.

However, the RNA-binding mutant of Bfr1p rescues the expression of Erg4p. Reduction in Erg4-yeGFP is not due to increased vacuolar protein degradation since deletion of *PEP4*, and encoding a major vacuolar peptidase does not rescue this phenotype (Fig. 4A). To determine whether Erg4p is expressed at low levels or not at all, cell lysates were fractionated to enrich for membrane and cytosolic fractions. Western blot analysis shows a weaker expression of Erg4-yeGFP in *bfr1Δ* cells as compared to wild type and a shift in its distribution from the membrane to the cytosolic fraction (Fig. 4C). Although *bfr1Δ* yeast shares several phenotypes with *scp160Δ* cells, including an increase in ploidy and premature P-body formation, deletion of *SCP160* does not affect Erg4p protein localization (Fig. 4A, lower panels). This suggests that the observed low expression of Erg4p is specific to cells lacking Bfr1p.

Proteins that are misfolded at the ER are modified by the ubiquitin-protein ligase Hrd1p to facilitate their retranslocation to the cytoplasm and degradation by the 26S proteasome in the ERAD (ER-Associated Degradation) pathway (Hampton 2002; Baldridge and Rappaport 2016). Because *ERG4* mRNA is translated at the ER, potentially misfolded Erg4p could be degraded by this pathway in *bfr1Δ* cells. We, therefore, generated a strain with a double deletion in *BFR1* and *HRD1* (*bfr1Δ hrd1Δ*) expressing Erg4p-yeGFP. We then blocked 26S proteasome function using MG132 and prepared cell lysates before or after blocking translation (30 and 60 min) by adding CHX. In western blots, we observed an increased accumulation of Erg4p upon MG132 treatment in *bfr1Δ and bfr1Δ hrd1Δ* cells, but the increase was much larger in the double deletion. This suggests that Erg4p is misfolded in cells lacking Bfr1p and targeted by the ERAD pathway (Fig. 4D). Thus, Bfr1p might help in proper translocation of Erg4p into the ER.

Bfr1p affects polysome association of *ERG4* mRNA

Because Bfr1p has been shown to associate with polysomes (Lang et al. 2001), we decided to test if Bfr1p directly interacts with ribosomes and if its interaction with mRNA occurs during translation. For this, we performed coimmunoprecipitation of a yeGFP-tagged Bfr1p and ribosomes, using the ribosomal small subunit protein Rps3p as a proxy. We found no evidence for Bfr1p to coimmunoprecipitate ribosomes (Fig. 5A, IP) and conclude that the interaction, if any, can only be weak or transient.

We next investigated if the loss of *BFR1* or mutations in its RNA-binding sites result in changes of translation of *ERG4*. We first addressed this by ribosomal affinity

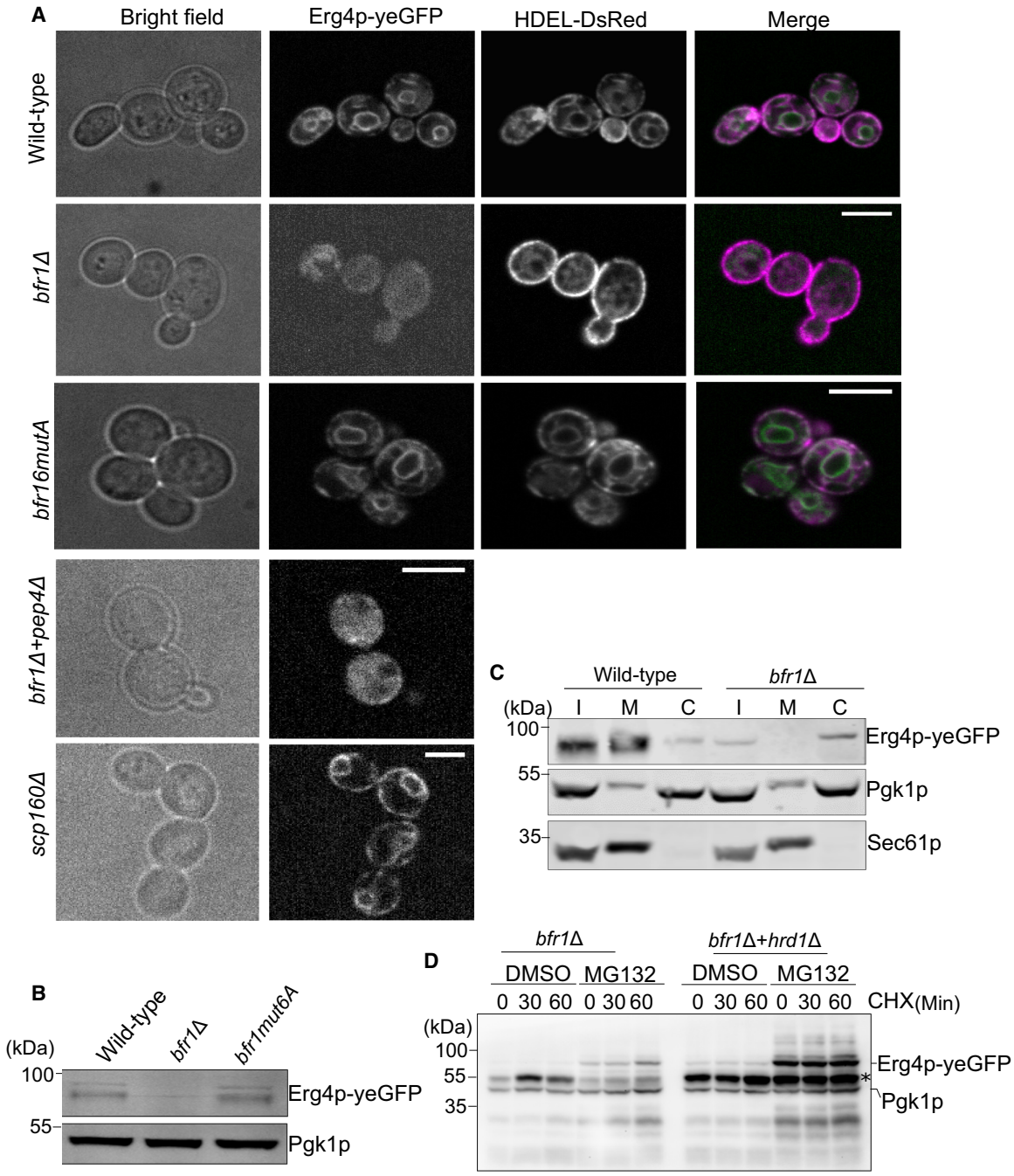

FIGURE 4. Bfr1p controls Erg4p expression and distribution. (*A*) Erg4p distribution changes upon deletion of *BFR1*. Representative images of cells from wild-type, *bfr1*Δ, *bfr1mut6A*, *bfr1*Δ *pep4*Δ, and *scp160*Δ strains. HDEL-DsRed serves as an ER marker. Scale bar, 5 µm. (*B*) Western blot showing down-regulation of Erg4p in *bfr1*Δ and *bfr1mut6A* compared to wild type. Total cell lysates were prepared from wild-type, *bfr1*Δ, and *bfr1mut6A* cells expressing a yeGFP-tagged Erg4p protein and Erg4p detected by an anti-GFP antibody. (*C*) Erg4p shifts from ER to cytoplasm in *bfr1*Δ cells. Western blot following subcellular fractionation of wild-type and *bfr1*Δ cells expressing yeGFP-tagged Erg4p. (I) input, (M) membrane fraction, pellet 18,000*g*, and (C) cytoplasmic fraction, supernatant 18,000*g*. Pgk1p and Sec61p serve as a cytoplasmic or ER marker, respectively. (*D*) Representative western blot showing accumulation of Erg4p in an ERAD mutant upon treatment with MG132. Total cell lysates were prepared from *bfr1*Δ and *bfr1*Δ *hrd1*Δ cells expressing yeGFP-tagged Erg4p. Cells were harvested at 0, 30, and 60 min after adding cycloheximide (CHX). Pgk1p served as a loading control. The asterisk indicates an unspecific band at 55 kDa detected by the GFP antibody.

purification in combination with mRNA detection by qRT-PCR (Hirschmann et al. 2014). Ribosomes and bound mRNAs were affinity-purified from CHX-treated cells via a TAP-tagged ribosomal Rpl16a protein. The level of ribosome-associated *OSH7*, *ACT1*, and *MID2* mRNAs in *bfr1Δ* cells is very similar to that of wild-type cells (Fig. 5B),

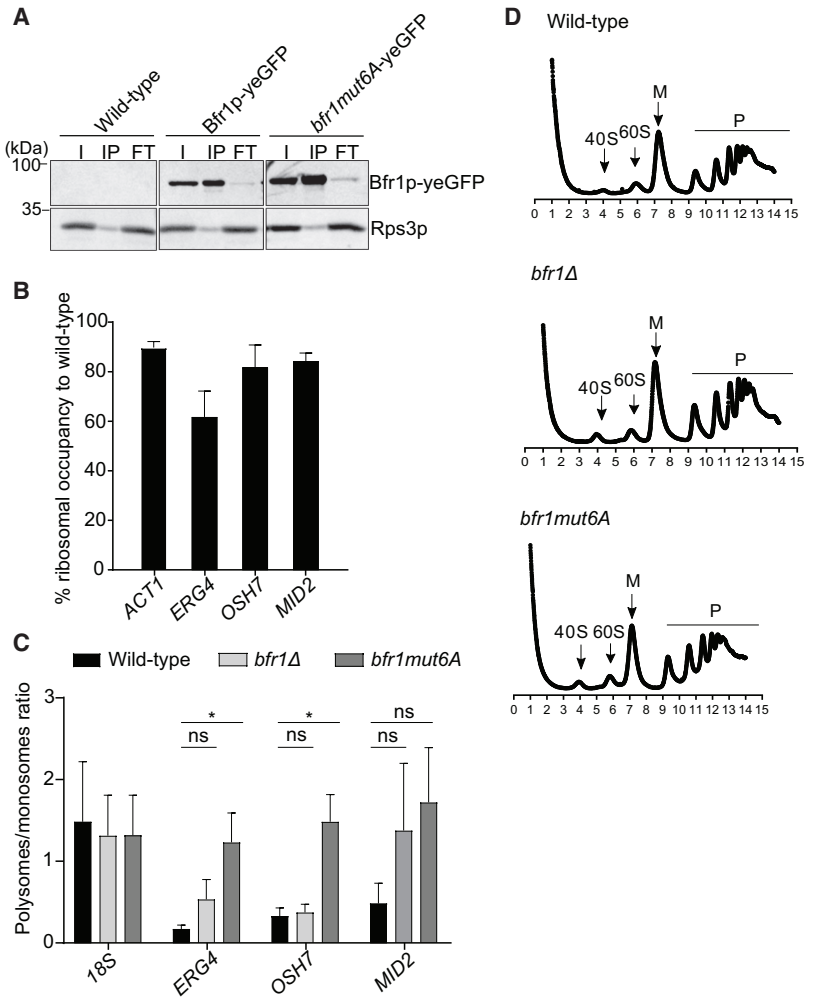

FIGURE 5. Bfr1p is required for efficient translational elongation of *ERG4* mRNA. (*A*) Bfr1p does not coprecipitate the small ribosomal subunit protein Rps3p indicating Bfr1p interaction with ribosomes is unstable. A representative image of three independent experiments from Bfr1p-yeGFP immunoprecipitations. (I) Input, (IP) immunoprecipitation, (FT) flowthrough. (*B*) Ribosomal occupancy of *ERG4* mRNA is reduced in the absence of Bfr1p. Ribosome affinity purification (RAP) followed by qRT-PCR was performed to measure the ribosome association of *ACT1*, *ERG4*, *OSH7*, and *MID2* mRNAs in wild-type and *bfr1*Δ cells. An untagged (mock) strain was used to normalize the data. Quantification graphs show percentage of occupancy in *bfr1*Δ to the wild-type levels in three biological and two technical replicates of each with ±SD. (*C*) Polysome association of *ERG4* mRNA changes in *bfr1mut6A* and *bfr1*Δ. Sucrose density gradient fractionation was used to separate monosomes and polysomes, and RNAs from the fractions were quantified by qRT-PCR. Results are displayed as the fold change ratio of polysomes/monosomes for four mRNAs (normalized to *ACT1* levels) from three independent experiments with ±SD. An asterisk indicates $P < 0.05$. (ns) Nonsignificant. (*D*) Polysome profiles from *bfr1mut6A* and *bfr1*Δ compared to wild-type cells. (M) monosomes, (P) polysomes.

indicating that their ribosomal occupancy is independent of Bfr1p. In contrast, the amount of ribosome-associated *ERG4* is reduced. Because this method cannot distinguish between monosome- or polysome-associated mRNAs, we applied polysome fractionation and determined the distribution of mRNAs between monosomes and polysomes, which can serve as a proxy for the translational efficiency of a given mRNA. Ribosome distribution between fractions containing free ribosomal subunits, monosomes, or polysomes is similar in wild-type, *bfr1Δ*, and *bfr1mut6A* cells, as judged by the polysome/monosome ratio of 18S rRNA (Fig. 5C) or polysome profiles (Fig. 5D). In contrast, significant changes were seen for the distribution of *ERG4* ($P < 0.0299$) and *OSH7* ($P < 0.0178$) between polysomes and monosomes when comparing wild-type cells and cells expressing the Bfr1p mutant *bfr1mut6A*. We also observed changes in the distribution of the control mRNA *MID2*, although with low significance ($P < 0.0708$). Polysome profiles show *ERG4* and *OSH7* mRNAs are increased in polysomes of *bfr1mut6A* compared to wild-type cells. Although this might suggest a better translation, which is in contrast to protein expression (Fig. 4B). This apparent discrepancy might be due to the presence of *ERG4* and *OSH7* mRNAs on stalled ribosomes or improper translocation of the proteins in *bfr1* mutants. A similar observation has been made in the case of Scp160p in which at least one of its target mRNAs, *PRY3*, is increased in polysomes in cells lacking Scp160p, whereas Pry3 protein expression is reduced (Hirschmann et al. 2014).

DISCUSSION

The yeast RBP Bfr1p has been implicated in various cellular functions, ranging from control of SPB duplication to P-body formation. Because Bfr1p binds to several hundred mRNAs and is found in the polysome fraction during sucrose gradient centrifugation, the multiple phenotypes associated with loss of *BFR1* might result from a function in translation or translation regulation. To establish additional evidence for this model and to investigate if the loss of RNA binding is causing the reported phenotypes associated with *BFR1* deletion, we studied the consequences of mutations in documented RNA-binding sites (Kramer et al. 2014). The mutated amino acids are conserved between several yeast species and are located in the first and second coiled-coil domain of Bfr1p as well as in the region connecting these two coiled-coils. Conversion of six of these RNA contact sites to alanines (*bfr1mut6A*) results in loss of the mRNA binding capacity

as shown for *ERG4* mRNA. As a consequence, the ER localization of Bfr1p is lost and the protein redistributes to the cytoplasm. This suggests that Bfr1p is targeted to ER in a piggyback manner via bound mRNAs that are translated at the cytoplasmic face of the ER. Among the six conserved RNA contact sites, phenylalanine 293 seems to be the most critical because the loss of ER association can also be seen for the F293A mutation. Surprisingly, although ER association is lost in these mutants, none of the other described phenotypes that have been described for *bfr1Δ* cells can be detected (Jackson and Képès 1994; Simpson et al. 2014; Weidner et al. 2014). Cells expressing *bfr1mut6A* do not show loss of ploidy control and stay haploid. Like wild-type *BFR1*, overexpression of *bfr1mut6A* can fully rescue an *erg6Δ* mutant when exposed to brefeldin A (Jackson and Képès 1994). Finally, unlike *bfr1Δ* cells, cells expressing the RNA-binding mutant do not show a premature formation of P-bodies in unstressed cells (Weidner et al. 2014). Thus, RNA binding does not seem to be important for Bfr1p's functions in ploidy control, repression of P-body formation, or brefeldin A resistance. Similarly, the third coiled-coil domain of Bfr1p, which does not contain any identified RNA contact site, is also dispensable for controlling P-body formation and ploidy. This suggests that these functions of Bfr1p are associated with its amino-terminal section but might be mediated by protein–protein rather than protein–RNA interactions.

A large fraction of Bfr1p target mRNAs encodes proteins translated at the ER (Lapointe et al. 2015). Several RBPs have been described that participate in or mediate mRNA association with the ER independent of translation or SRP-mediated targeting (Cui and Palazzo 2014). These include mammalian p180 and Kinectin (Cui 2012) and the yeast RBPs She2p (Schmid et al. 2006) or Khd1p (Syed et al. 2018). In contrast to these, Bfr1p is not required for ER localization of at least one of its bound mRNAs, *ERG4*. In this respect, it mimics Scp160p, with which it shares its polysome association and ER colocalization. Although not necessary for mRNA localization, Bfr1p is required for the proper translation of the encoded Erg4 protein, which is consistent with its binding to translating polyribosomes (Fig. 5A,B; Lang et al. 2001). Not only is the total amount of Erg4 protein lower in *bfr1Δ* cells but the distribution of this membrane protein is altered and enriched in the cytosol rather than the membrane fraction. Erg4p catalysis is the final step of ergosterol synthesis from 5,7,22,24(28)-ergostatetraenol to ergosta-5,7,22-trien-3beta-ol. However, despite the observed altered protein distribution, we have not detected changes in the ergosterol level of *bfr1Δ* cells versus wild-type cells. It is thus likely that the remaining amounts of properly translated and targeted Erg4p suffices for ergosterol synthesis.

Concomitant with a postulated role of Bfr1p in the translation of *ERG4* mRNA, we also observed a decrease of the fraction of *ERG4* mRNA that copurifies with ribosomes. Surprisingly, the ratio of *ERG4* mRNA on polysomes versus monosomes increases, which is apparently contradictory to the findings of reduced translation. However, a similar observation has been made for cells lacking the conserved RBP Scp160p, although for a different set of mRNAs (Hirschmann et al. 2014). The reduced association of certain tRNAs with translating ribosomes in cells lacking Scp160p has led to the model that Scp160p is required for efficient translation of specific mRNA subsets and that its loss results in pausing or stalling of ribosomes on mRNAs (Hirschmann et al. 2014). We envision that Bfr1p might function similarly to Scp160p but might be important for regulating a different set of mRNAs encoding membrane or secreted proteins at ER.

MATERIALS AND METHODS

Yeast strains and plasmids

Generation of yeast strains and plasmids used in this study as well as general methods including cell lysis and subcellular fractionation are described in Supplemental Methods.

Confocal microscopy

In vivo imaging of fluorescent labeled proteins was carried out from inoculation of single colonies into SC or SDC medium containing 2% glucose and overnight growth at 30°C. Logarithmically growing cells were harvested and resuspended in 100 µL of fresh medium. Cells were spread on thin agarose pads containing SC or SDC with 2% glucose and grown for 30 min at 30°C before observing in the microscope (ZEISS AxioExaminer equipped with a CSU spinning disc confocal unit; Visitron Systems). Images were acquired with a 63× oil objective using VisiView software (Visitron Systems). Post-image processing was performed using Fiji software as described in Syed et al. (2018) and Hermesh et al. (2014). For *ERG4* mRNA localization, images were acquired, with each containing at least 60 cells. For P-body analysis, logarithmically growing cells were harvested, washed once with sterile water, and then cells were spread on agarose pads containing SDC medium without glucose and grown for 30 min at 30°C to induce P-bodies.

Coimmunoprecipitations

For protein–mRNA coprecipitations, experiments were performed as described in Syed et al. (2018) with the following changes. One hundred OD_{600} units of cells were harvested and resuspended in 8–10 µL/OD_{600} of lysis buffer (10 mM Tris-HCl pH 7.5, 150 mM NaCl, 2 mM EDTA, 0.1% Triton X-100, 1× Protease inhibitor cocktail and 0.5 U/µL Ribolock RNase inhibitor). Glass bead lysis was performed and cell debris was removed by 5 min centrifugation at 5000*g* at 4°C. Protein concentrations were measured and 200 µg of lysates were subjected to immunoprecipitation with GFP-Trap_MA magnetic beads (Chromotek) for 2 h at 4°C on a rotating wheel. The beads were blocked prior to the immunoprecipitations with blocking buffer (10 mM Tris-HCl pH

7.5, 150 mM NaCl, 2 mM EDTA, 0.1% Triton X-100, 0.1 mg/mL *Escherichia coli* tRNA and 0.4 mg/mL Heparin). Captured beads were washed 3× with 500 µL of wash buffer (10 mM Tris-HCl pH 7.5, 150 mM NaCl, 2 mM EDTA, and 0.1% Triton X-100) and resuspended beads with 125 µL of HPLC-grade water (Sigma-Aldrich). Seventy-five microliters of the bead slurry was used for SDS-PAGE and western blotting. RNA extraction was carried out with the remaining 50 µL of beads, to which 50 ng of spike RNA (in vitro transcribed *Arabidopsis* phosphoribulo kinase RNA) had been added. For extraction 5 µL of 3 M sodium acetate pH 5.2, 2.5 µL of 20% SDS and 50 µL of phenol/chloroform/isoamylalcohol (PCI) pH 4.5 was added and the mixed sample centrifuged at maximum speed for 30 min at 4°C. Nucleic acids were precipitated overnight at −80°C with 20 µg of glycogen and 100 µL of 96% ethanol, and RNA was resuspended in 20 µL of RNase-free water before continuing with cDNA synthesis and qPCR.

For coimmunoprecipitation of Rps3p, captured beads were washed 3× with 500 µL of wash buffer, and bound proteins were eluted by adding 1× SDS sample buffer to the beads and boiled for 5 min at 95°C and proceeded with SDS-PAGE and western blot analysis.

RNA extraction, RT-PCR, and qRT-PCR

Total RNA was extracted from 20 OD_{600} units of yeast strains RJY358 and RJY4626. Glass beads lysis was performed in 500 µL of Cross buffer I (0.3 M NaCl, 10 mM Tris-what pH 7.5, 1 mM EDTA, 0.2% SDS) and 400 µL of phenol:chloroform:isoamylalcohol by four pulses of 120 sec with breaks of 60 sec on ice. After centrifugation for 30 min at full speed, the upper phase was transferred to a new tube and nucleic acids precipitated with ethanol for 30 min at −20°C. Total RNA pellets were washed and resuspended in 20 µL of HPLC-grade water before proceeding to cDNA synthesis and qPCR.

Reverse transcription reactions for all the experiments were performed as described in Syed et al. (2018) with some modifications. In brief, 1 µg of RNA samples were treated with RQ1 DNase (Promega), and reverse transcription reactions were performed using the High-Capacity cDNA Reverse Transcription Kit (Applied Biosystems). Quantitative RT-PCR (qRT-PCR) was performed in 10 µL reactions containing 2.5 µL of cDNA samples at 1:25 or 1:50 dilutions. Target-specific primers were designed with Primer3 software (Rozen and Skaletsky 2000). All reactions were performed from a minimum of three biological replicates and two technical replicates of each. Quantification was performed by the comparative ΔΔCt method (Livak and Schmittgen 2001; Syed et al. 2018), and values were normalized via the spiked-in RNA or via *ACT1* mRNA signals. For the RT-PCR reactions after RNAse treatment, a PCR reaction with 1 µL of cDNA with dilutions up to 1:1000 was performed using Taq DNA polymerase (Genaxxon Bioscience). PCR was performed for 18 cycles using primers specific to *18S* rRNA and *ERG4* mRNA, and amplified products were separated by 1% agarose gel electrophoresis.

Ribosome affinity purifications (RAP-IP)

Ribosome affinity purification (RAP-IP) to determine *ERG4* and *OSH7* mRNAs bound to ribosomes was performed as described in Hirschmann et al. (2014). For the quantifications of mRNAs bound to the ribosomes, qRT-PCR was performed, and the enrichment of mRNAs was determined using the ΔΔCT method. An enrichment of mRNAs from TAP purification (in wild-type and *bfr1Δ*) was considered only if at least twofold greater than from mock purification (strains without TAP tags). The percentage ribosomal occupancy of *bfr1Δ* was then plotted against wild-type levels for the *ACT1*, *ERG4*, *MID2*, and *OSH7* mRNAs (Fig. 5C).

Brefeldin A sensitivity drop assay

A single colony of yeast cells was inoculated and grown overnight before diluting it into fresh medium to grow until logarithmic phase. Cells were harvested and washed once with sterile water. One OD_{600} unit of cells was used for serial dilution and 3 µL of dilutions were plated on SDC-leu medium with or without 50 µg/mL of brefeldin A (eBioscience). Cells were grown for 72 h at 30°C.

Ploidy analysis by flow cytometry

Cells were prepared for flow cytometry analysis as described (Baum et al. 2004; Hirschmann et al. 2014). Propidium iodide fluorescence was detected in a Beckman Coulter CytoFlex LX system with a 675/30 nm filter. Data were analyzed using CytExpert software (Beckman Coulter), and representative graphs were plotted manually using values obtained from the software.

Proteasome inhibition by MG132

To block the proteasomes, we have used commercially available proteasome inhibitor MG132 (Sigma-Aldrich) and permeabilized into the cells as described in Liu et al. (2007). Briefly, single colony cells were inoculated overnight in a synthetic medium containing 0.17% yeast nitrogenous base without ammonium sulfate and supplemented with 0.1% proline, appropriate amino acids, and 2% glucose as the carbon source. Cultures were reinoculated in fresh 30 mL media with 0.003% of SDS for 3 h at 30°C. Then 75 µM MG132 dissolved in DMSO or DMSO alone as a control was added to the cultures and grown for 30 min at 30°C before adding 100 µg/mL of CHX to the cultures to stop the translation. Cells were harvested at 0, 30, and 60 min and proceeded with cell lysis and western blot to analyze the protein levels.

Polysome profiling

Separation of mono and polysomes was done as described in Mittal et al. (2017) and performed with three biological replicates of wild-type, *bfr1Δ*, and *bfr1mut6A* strains. Logarithmically growing cells were treated with 100 µg/mL CHX for 1 min, harvested by vacuum filtration, and flash-frozen with liquid nitrogen. Cells lysis was performed under cryogenic conditions using lysis buffer (20 mM Tris-HCl, pH 7.5, 100 mM NaCl, 10 mM $MgCl_2$, 1% Triton X-100, 0.5 mM DDT, and 100 µg/mL of CHX) and a bead mill (Spex Inc.). Cell debris was removed by centrifugation for 3 min at 3000*g* and 4°C followed by 10,000*g* for 5 min at 4°C. To separate monosomes and polysomes, 10 A_{260} units of lysates were loaded on precooled 12 mL of 7%–47% linear sucrose gradients (50 mM Tris-HCl, pH 7.5, 50 mM NH_4Cl, 12 mM $MgCl_2$, 0.5 mM

DTT, and 100 µg/mL CHX) and centrifuged at 35,000 rpm for 3 h at 4°C in a TH-641 rotor (Thermo Scientific) before collecting the monosome and polysome peaks (Fig. 5D). RNA was isolated by adding 5 µL of glycogen and phenol:chloroform (5:1) before reextraction of the aqueous phase with chloroform and precipitation in ethanol overnight at −20°C. RNA pellets were resuspended in 30 µL of HPLC-grade water and processed for cDNA synthesis and qRT-PCR.

SUPPLEMENTAL MATERIAL

Supplemental material is available for this article.

ACKNOWLEDGMENTS

We are thankful to Robert H. Singer and Roy Parker for providing plasmids MCPNLSSV40-2x-yeGFP and Edc3-mCherry, respectively. We are grateful to Syed Muhammad Ibrahim for helping with subcellular fractionation, microscopy experiments, and providing spike RNA. Joyita Mukherjee helped in data analysis of qRT-PCR and coimmunoprecipitation experiments. Mathew Cheng is thanked for suggestions on the manuscript.

Author contributions: S.M. and R.-P.J. designed research; S.M. performed the research and analyzed data; S.M. and N.M. performed polysome profiling; N.M. and A.S. provided reagents; S.M., A.S., and R.-P.J. wrote the manuscript.

Received May 20, 2019; accepted August 20, 2019.

REFERENCES

Auweter SD, Oberstrass FC, Allain FH-T. 2006. Sequence-specific binding of single-stranded RNA: is there a code for recognition? *Nucleic Acids Res* **34:** 4943–4959. doi:10.1093/nar/gkl620

Baldridge RD, Rapoport TA. 2016. Autoubiquitination of the Hrd1 ligase triggers protein retrotranslocation in ERAD. *Cell* **166:** 394–407. doi:10.1016/j.cell.2016.05.048

Baltz AG, Munschauer M, Schwanhäusser B, Vasile A, Murakawa Y, Schueler M, Youngs N, Penfold-Brown D, Drew K, Milek M, et al. 2012. The mRNA-bound proteome and its global occupancy profile on protein-coding transcripts. *Mol Cell* **46:** 674–690. doi:10.1016/j.molcel.2012.05.021

Baum S, Bittins M, Frey S, Seedorf M. 2004. Asc1p, a WD40-domain containing adaptor protein, is required for the interaction of the RNA-binding protein Scp160p with polysomes. *Biochem J* **380:** 823–830. doi:10.1042/bj20031962

Beckmann BM, Horos R, Fischer B, Castello A, Eichelbaum K, Alleaume A-M, Schwarzl T, Curk T, Foehr S, Huber W, et al. 2015. The RNA-binding proteomes from yeast to man harbour conserved enigmRBPs. *Nat Commun* **6:** 10127. doi:10.1038/ncomms10127

Beh CT, Cool L, Phillips J, Rine J. 2001. Overlapping functions of the yeast oxysterol-binding protein homologues. *Genetics* **157:** 1117–1140.

Bevis BJ, Glick BS. 2002. Rapidly maturing variants of the *Discosoma* red fluorescent protein (DsRed). *Nat Biotechnol* **20:** 83–87. doi:10.1038/nbt0102-83

Björk P, Wieslander L. 2017. Integration of mRNP formation and export. *Cell Mol Life Sci* **74:** 2875–2897. doi:10.1007/s00018-017-2503-3

Castello A, Fischer B, Eichelbaum K, Horos R, Beckmann BM, Strein C, Davey NE, Humphreys DT, Preiss T, Steinmetz LM, et al. 2012. Insights into RNA biology from an atlas of mammalian mRNA-binding proteins. *Cell* **149:** 1393–1406. doi:10.1016/j.cell.2012.04.031

Castello A, Hentze MW, Preiss T. 2015. Metabolic enzymes enjoying new partnerships as RNA-binding proteins. *Trends Endocrinol Metab* **26:** 746–757. doi:10.1016/j.tem.2015.09.012

Castello A, Fischer B, Frese CK, Horos R, Alleaume A-M, Foehr S, Curk T, Krijgsveld J, Hentze MW. 2016. Comprehensive identification of RNA-binding domains in human cells. *Mol Cell* **63:** 696–710. doi:10.1016/j.molcel.2016.06.029

Cui XA, Palazzo AF. 2014. Localization of mRNAs to the endoplasmic reticulum. *Wiley Interdiscip Rev RNA* **5:** 481–492. doi:10.1002/wrna.1225

Cui XA, Zhang H, Palazzo AF. 2012. p180 promotes the ribosome-independent localization of a subset of mRNA to the endoplasmic reticulum. *PLOS Biol* **10:** e1001336. https://doi.org/10.1371/journal.pbio.1001336

Dreyfuss G, Kim VN, Kataoka N. 2002. Messenger-RNA-binding proteins and the messages they carry. *Nat Rev Mol Cell Biol* **3:** 195–205. doi:10.1038/nrm760

Entian K-D, Schuster T, Hegemann JH, Becher D, Feldmann H, Güldener U, Götz R, Hansen M, Hollenberg CP, Jansen G, et al. 1999. Functional analysis of 150 deletion mutants in *Saccharomyces cerevisiae* by a systematic approach. *Mol Gen Genet* **262:** 683–702. doi:10.1007/PL00013817

Fundakowski J, Hermesh O, Jansen R-P. 2012. Localization of a subset of yeast mRNAs depends on inheritance of endoplasmic reticulum. *Traffic* **13:** 1642–1652. doi:10.1111/tra.12011

Gillingham AK, Munro S. 2003. Long coiled-coil proteins and membrane traffic. *Biochim Biophys Acta* **1641:** 71–85. doi:10.1016/S0167-4889(03)00088-0

Graham TR, Scott PA, Emr SD. 1993. Brefeldin A reversibly blocks early but not late protein transport steps in the yeast secretory pathway. *EMBO J* **12:** 869–877. doi:10.1002/j.1460-2075.1993.tb05727.x

Hampton RY. 2002. ER-associated degradation in protein quality control and cellular regulation. *Curr Opin Cell Biol* **14:** 476–482. doi:10.1016/S0955-0674(02)00358-7

Hasegawa Y, Irie K, Gerber AP. 2008. Distinct roles for Khd1p in the localization and expression of bud-localized mRNAs in yeast. *RNA* **14:** 2333–2347. doi:10.1261/rna.1016508

Hentze MW, Castello A, Schwarzl T, Preiss T. 2018. A brave new world of RNA-binding proteins. *Nat Rev Mol Cell Biol* **19:** 327–341. doi:10.1038/nrm.2017.130

Hermesh O, Genz C, Yofe I, Sinzel M, Rapaport D, Schuldiner M, Jansen R-P. 2014. Yeast phospholipid biosynthesis is linked to mRNA localization. *J Cell Sci* **127:** 3373–3381. doi:10.1242/jcs.149799

Hirschmann WD, Westendorf H, Mayer A, Cannarozzi G, Cramer P, Jansen R-P. 2014. Scp160p is required for translational efficiency of codon-optimized mRNAs in yeast. *Nucleic Acids Res* **42:** 4043–4055. doi:10.1093/nar/gkt1392

Hogan DJ, Riordan DP, Gerber AP, Herschlag D, Brown PO. 2008. Diverse RNA-binding proteins interact with functionally related sets of RNAs, suggesting an extensive regulatory system. *PLoS Biol* **6:** e255. doi:10.1371/journal.pbio.0060255

Jackson CL, Képès F. 1994. BFR1, a multicopy suppressor of brefeldin A–induced lethality, is implicated in secretion and nuclear segregation in *Saccharomyces cerevisiae*. *Genetics* **137:** 423–437.

Jan CH, Williams CC, Weissman JS. 2014. Principles of ER cotranslational translocation revealed by proximity-specific ribosome profiling. *Science* **346:** 1257521. doi:10.1126/science.1257521

Kramer K, Sachsenberg T, Beckmann BM, Qamar S, Boon K-L, Hentze MW, Kohlbacher O, Urlaub H. 2014. Photo-cross-linking and high-resolution mass spectrometry for assignment of RNA-binding sites in RNA-binding proteins. *Nat Methods* **11:** 1064–1070. doi:10.1038/nmeth.3092

Kwon SC, Yi H, Eichelbaum K, Föhr S, Fischer B, You KT, Castello A, Krijgsveld J, Hentze MW, Kim VN. 2013. The RNA-binding protein repertoire of embryonic stem cells. *Nat Struct Mol Biol* **20:** 1122–1130. doi:10.1038/nsmb.2638

Lai MH, Bard M, Pierson CA, Alexander JF, Goebl M, Carter GT, Kirsch DR. 1994. The identification of a gene family in the *Saccharomyces cerevisiae* ergosterol biosynthesis pathway. *Gene* **140:** 41–49. doi:10.1016/0378-1119(94)90728-5

Lang BD, Fridovich-Keil JL. 2000. Scp160p, a multiple KH-domain protein, is a component of mRNP complexes in yeast. *Nucleic Acids Res* **28:** 1576–1584. doi:10.1093/nar/28.7.1576

Lang BD, Am L, Black-Brewster HD, Fridovich-Keil JL. 2001. The brefeldin A resistance protein Bfr1p is a component of polyribosome-associated mRNP complexes in yeast. *Nucleic Acids Res* **29:** 2567–2574. doi:10.1093/nar/29.12.2567

Lapointe CP, Wilinski D, Saunders HAJ, Wickens M. 2015. Protein–RNA networks revealed through covalent RNA marks. *Nat Methods* **12:** 1163–1170. doi:10.1038/nmeth.3651

Lewis HA, Musunuru K, Jensen KB, Edo C, Chen H, Darnell RB, Burley SK. 2000. Sequence-specific RNA binding by a Nova KH domain: implications for paraneoplastic disease and the fragile X syndrome. *Cell* **100:** 323–332. doi:10.1016/S0092-8674(00)80668-6

Liu C, Apodaka J, Davis LE, Rao H. 2007. Proteasome inhibition in wild-type yeast *Saccharomyces cerevisiae* cells. *Biotechniques* **42:** 158–162. doi:10.2144/000112389

Livak KJ, Schmittgen TD. 2001. Analysis of relative gene expression data using real-time quantitative PCR and the $2^{-\Delta\Delta CT}$ method. *Methods* **25:** 402–408. doi:10.1006/meth.2001.1262

Loewen CJR, Young BP, Tavassoli S, Levine TP. 2007. Inheritance of cortical ER in yeast is required for normal septin organization. *J Cell Biol* **179:** 467–483. doi:10.1083/jcb.200708205

Low YS, Bircham PW, Maass DR, Atkinson PH. 2014. Kinetochore genes are required to fully activate secretory pathway expansion in *S. cerevisiae* under induced ER stress. *Mol Biosyst* **10:** 1790–1802. doi:10.1039/c3mb70414a

Lu D, Searles MA, Klug A. 2003. Crystal structure of a zinc-finger-RNA complex reveals two modes of molecular recognition. *Nature* **426:** 96–100. doi:10.1038/nature02088

Lunde BM, Moore C, Varani G. 2007. RNA-binding proteins: modular design for efficient function. *Nat Rev Mol Cell Biol* **8:** 479–490. doi:10.1038/nrm2178

Mitchell SF, Jain S, She M, Parker R. 2013. Global analysis of yeast mRNPs. *Nat Struct Mol Biol* **20:** 127–133. doi:10.1038/nsmb.2468

Mittal N, Guimaraes JC, Gross T, Schmidt A, Vina-Vilaseca A, Nedialkova DD, Aeschimann F, Leidel SA, Spang A, Zavolan M. 2017. The Gcn4 transcription factor reduces protein synthesis capacity and extends yeast lifespan. *Nat Commun* **8:** 457. doi:10.1038/s41467-017-00539-y

Neriec N, Percipalle P. 2018. Sorting mRNA molecules for cytoplasmic transport and localization. *Front Genet* **9:** 510. doi:10.3389/fgene.2018.00510

Oubridge C, Ito N, Evans PR, Teo C-H, Nagai K. 1994. Crystal structure at 1.92 Å resolution of the RNA-binding domain of the U1A spliceosomal protein complexed with an RNA hairpin. *Nature* **372:** 432–438. doi:10.1038/372432a0

Rozen S, Skaletsky H. 2000. Primer3 on the WWW for general users and for biologist programmers. In *Bioinformatics methods and protocols. Methods in molecular biology* (ed. Misener S, Krawetz SA), Vol. 132. Humana Press, Totowa, NJ. https://doi.org/10.1385/1-59259-192-2:365.

Ryter JM, Schultz SC. 1998. Molecular basis of double-stranded RNA–protein interactions: structure of a dsRNA-binding domain complexed with dsRNA. *EMBO J* **17:** 7505–7513. doi:10.1093/emboj/17.24.7505

Setty SRG, Shin ME, Yoshino A, Marks MS, Burd CG. 2003. Golgi recruitment of GRIP domain proteins by Arf-like GTPase 1 is regulated by Arf-like GTPase 3. *Curr Biol* **13:** 401–404. doi:10.1016/S0960-9822(03)00089-7

Sezen B, Seedorf M, Schiebel E. 2009. The SESA network links duplication of the yeast centrosome with the protein translation machinery. *Genes Dev* **23:** 1559–1570. doi:10.1101/gad.524209

Schmid M, Jaedicke A, Du T-G, Jansen R-P. 2006. Coordination of endoplasmic reticulum and mRNA localization to the yeast bud. *Curr Biol* **16:** 1538–1543. doi:10.1016/j.cub.2006.06.025

Shah N, Klausner RD. 1993. Brefeldin A reversibly inhibits secretion in *Saccharomyces cerevisiae*. *J Biol Chem* **268:** 5345–5348.

Simpson CE, Lui J, Kershaw CJ, Sims PFG, Ashe MP. 2014. mRNA localization to Pbodies in yeast is biphasic with many mRNAs captured in a late Bfr1pdependent wave. *J Cell Sci* **127:** 1254–1262. doi:10.1242/jcs.139055

Syed MI, Moorthy BT, Jenner A, Fetka I, Jansen R-P. 2018. Signal sequence-independent targeting of *MID2* mRNA to the endoplasmic reticulum by the yeast RNA-binding protein Khd1p. *FEBS Lett* **592:** 1870–1881. doi:10.1002/1873-3468.13098

Tutucci E, Vera M, Biswas J, Garcia J, Parker R, Singer RH. 2018. An improved MS2 system for accurate reporting of the mRNA life cycle. *Nat Methods* **15:** 81. doi:10.1038/nmeth.4502

Weidner J, Wang C, Prescianotto-Baschong C, Estrada AF, Spang A. 2014. The polysome-associated proteins Scp160 and Bfr1 prevent P body formation under normal growth conditions. *J Cell Sci* **127:** 1992–2004. doi:10.1242/jcs.142083

Xue Z, Shan X, Sinelnikov A, Mélèse T. 1996. Yeast mutants that produce a novel type of ascus containing asci instead of spores. *Genetics* **144:** 979–989.

Zweytick D, Hrastnik C, Kohlwein SD, Daum G. 2000. Biochemical characterization and subcellular localization of the sterol C-24(28) reductase, erg4p, from the yeast *saccharomyces cerevisiae*. *FEBS Lett* **470:** 83–87. doi:10.1016/S0014-5793(00)01290-4